Journal of Biomechanics 43 (2010) 1401–1407

Contents lists available at ScienceDirect

Journal of Biomechanics

journal homepage: www.elsevier.com/locate/jbiomech
www.JBiomech.com

Joint kinetic response during unexpectedly reduced plantar flexor torque provided by a robotic ankle exoskeleton during walking☆,☆☆

Pei-Chun Kao [a,*], Cara L. Lewis [b], Daniel P. Ferris [a]

[a] School of Kinesiology, University of Michigan, Ann Arbor, MI 48109-2214, USA
[b] College of Health & Rehabilitation Sciences: Sargent College, Boston University, Boston, MA 02215, USA

ARTICLE INFO

Article history:
Accepted 22 December 2009

Keywords:
Gait
Powered orthosis
H-reflex
Locomotion
Inverse dynamics
Joint kinetics
EMG

ABSTRACT

During human walking, plantar flexor activation in late stance helps to generate a stable and economical gait pattern. Because plantar flexor activation is highly mediated by proprioceptive feedback, the nervous system must modulate reflex pathways to meet the mechanical requirements of gait. The purpose of this study was to quantify ankle joint mechanical output of the plantar flexor stretch reflex response during a novel unexpected gait perturbation. We used a robotic ankle exoskeleton to mechanically amplify the ankle torque output resulting from soleus muscle activation. We recorded lower-body kinematics, ground reaction forces, and electromyography during steady-state walking and during randomly perturbed steps when the exoskeleton assistance was unexpectedly turned off. We also measured soleus Hoffmann- (H-) reflexes at late stance during the two conditions. Subjects reacted to the unexpectedly decreased exoskeleton assistance by greatly increasing soleus muscle activity about 60 ms after ankle angle deviated from the control condition ($p<0.001$). There were large differences in ankle kinematic and electromyography patterns for the perturbed and control steps, but the total ankle moment was almost identical for the two conditions ($p=0.13$). The ratio of soleus H-reflex amplitude to background electromyography was not significantly different between the two conditions ($p=0.4$). This is the first study to show that the nervous system chooses reflex responses during human walking such that invariant ankle joint moment patterns are maintained during perturbations. Our findings are particularly useful for the development of neuromusculoskeletal computer simulations of human walking that need to adjust reflex gains appropriately for biomechanical analyses.

1. Introduction

To generate a stable and economical gait pattern, it is critical to activate ankle plantar flexor muscles with the correct timing and appropriate magnitude to produce trailing limb push-off during late stance. A powered walking model by Kuo indicates that push-off performed along the trailing leg immediately before heel strike of the leading leg is four times less costly than driving the stance leg with hip mechanical power at other time points during the gait cycle (Kuo, 2002). In humans, the ankle mechanical power burst provides the majority of positive work required to restore the energy lost in redirecting the center of mass in step-to-step transitions (Kuo and Donelan et al., 2005). In addition to the correct timing, adequate magnitude of ankle push-off is necessary to reduce energy loss due to collision in the leading leg. These two factors, timing and magnitude of ankle push-off, may be used to explain why many pathological gaits exhibit high metabolic costs (Sawicki et al., 2009).

As plantar flexor muscle activity is largely mediated by proprioceptive feedback during walking (Yang et al., 1991; Sinkjaer et al., 1996; Nielsen and Sinkjaer, 2002; Mazzaro et al., 2005a; Mazzaro et al., 2005b; Rossignol et al., 2006; af Klint et al., 2008, 2009), it is important that the nervous system modulates stretch reflex pathways to meet the mechanical requirements of gait. Thus, well-modulated reflex responses play an important role in correcting gait perturbations and preventing falling by rapidly regulating motor neuron discharge (Nielsen and Sinkjaer, 2002). Previous studies have shown sudden increases in ankle plantar flexor electromyographic (EMG) activation following a perturbation that rapidly dorsiflexes the ankle during walking

☆Supported by the National Institutes of Health (R21 NS062119 to DPF, F32 HD055010 to CLL).

☆☆The study was partially published as an abstract in the Proceedings of the North American Congress on Biomechanics (Ann Arbor, Michigan, 2008) and the 33rd Annual Meeting of the American Society of Biomechanics (State College, Pennsylvania, 2009).

* Correspondence to: 301 McKinly Laboratory, University of Delaware, Newark, DE 19716, USA. Tel.: +1 302 831 8666; fax: +1 302 831 4234.
E-mail address: kaop@udel.edu (P.-C. Kao).

0021-9290/$ - see front matter © 2010 Elsevier Ltd. All rights reserved.
doi:10.1016/j.jbiomech.2009.12.024

(Yang et al., 1991; Sinkjaer et al., 1996). The stretch reflex increases ankle plantar flexor activation, augmenting the ankle plantar flexor moment and keeping the lower limb from collapsing when an external perturbation is encountered.

Measurements of joint mechanics during the stretch reflex responses to gait perturbation are necessary to add accurate reflexes to musculoskeletal computer simulations of gait. Adding reflexes to the models allows for a more physiologically realistic simulation (Pandy, 2001; Pearson et al., 2006), especially when the simulation dynamics involve responses to external perturbations. Most current musculoskeletal computer simulations of gait lack physiologically based reflex responses. They often use predetermined limb trajectories and joint kinetics from experimental data, and/or implement optimization routines for some objective features of gait (e.g. minimizing deviation of the trunk from upright posture) (Gilchrist and Winter, 1997).

We have a limited understanding of how stretch reflex responses directly impact joint mechanical output during human walking. Past studies on plantar flexor reflex response to perturbations have focused on muscle activation and joint kinematics (Yang et al., 1991; Sinkjaer et al., 1996; Nielsen and Sinkjaer, 2002; Mazzaro et al., 2005a; Mazzaro et al., 2005b; Rossignol et al., 2006; af Klint et al., 2008, 2009). It is not clear if there is a kinetic goal for the nervous system in modulating reflex responses during gait. As muscle activation increases during a perturbation because of the reflex response, does the response maintain joint moments to a level similar to unperturbed gait?

The purpose of this study was to mechanically quantify joint kinetics of reflex responses during an unexpected gait perturbation. Previous studies on motor adaptation to a robotic ankle exoskeleton found that subjects decreased soleus EMG amplitude by 28–35% when walking with exoskeleton plantar flexor assistance (Gordon and Ferris, 2007; Sawicki and Ferris, 2008). It seemed likely that turning off the robotic assistance unexpectedly after adaptation would cause a gait perturbation and result in a reflex response stabilizing the body. We examined neurologically intact subjects that had trained with the robotic ankle exoskeleton. In addition to kinematics and kinetics of their reflex responses, we also recorded soleus Hoffmann (H-) reflexes at late stance.

2. Methods

2.1. Subjects

Eleven healthy, neurologically intact subjects (5 male, 6 female; mass 71.6 ± 14.3 kg, mean ± SD) gave written informed consent and participated in this study. The University of Michigan Medical School Institutional Review Board approved the protocol, and the study conformed to the standards set by the Declaration of Helsinki.

2.2. Experimental design

We constructed a custom-made exoskeleton (Fig. 1) for the left lower limb of each subject. The ankle exoskeleton consisted of a carbon fiber shank section and a polypropylene foot section. A metal hinge between the sections allowed free sagittal plane rotation of the ankle joint. Two artificial pneumatic muscles attached to the posterior of the exoskeleton provided plantar flexor torque. We implemented proportional myoelectric control of the artificial muscles through a desktop computer and real-time control board (dSPACE Inc., Wixom, MI, USA) (Ferris et al., 2006; Gordon and Ferris, 2007). A custom real-time computer controller regulated air pressure in the artificial plantar flexor muscles proportional to the processed soleus electromyographic (EMG) signals via a pressure regulator. The EMG signals from the soleus were high-pass filtered with a second-order Butterworth filter (20 Hz cutoff frequency) to remove movement artifact, full wave rectified, and low-pass filtered with a second-order Butterworth filter (10 Hz cutoff frequency) to smooth the signal. We used a footswitch (B&L Engineering, Santa Ana, CA, USA) in the left shoe to detect heel strikes and calculate average gait cycle.

Before testing the motor response to the unexpectedly reduced ankle plantar flexor torque, subjects had completed two 30 min treadmill training sessions for

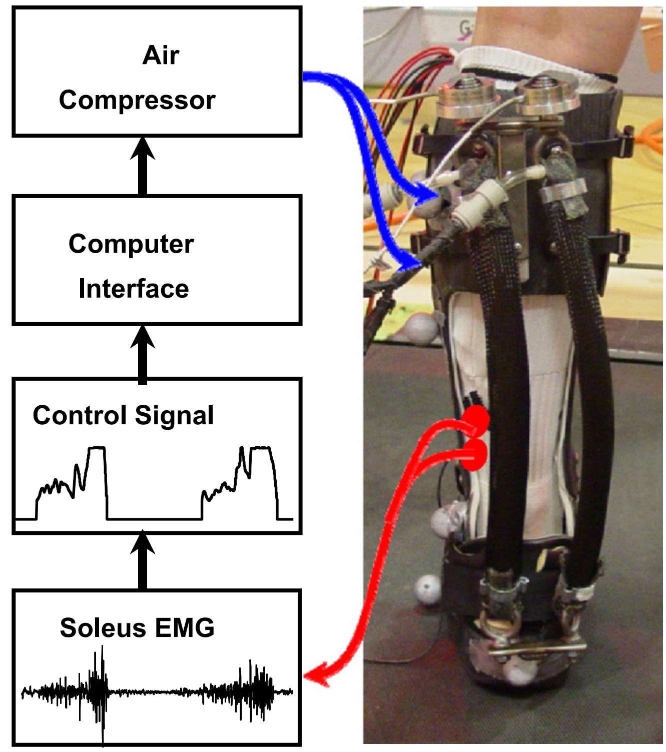

Fig. 1. Subjects wore a custom fit exoskeleton on their left lower limb. The exoskeleton was hinged at the ankle to allow free sagittal plane rotation. The exoskeleton had an average weight of 1.08 ± 0.09 kg (mean ± SD) and moment arm length of 11.0 ± 1.2 cm that varied and depended on the size of the subject. Electrical signals (EMG) of soleus activation were recorded and processed to be used to control air pressure in the artificial pneumatic muscles proportionally. As air pressure increased, the artificial muscles started to develop tension and become shortened, allowing the powered exoskeleton to provide plantar flexor torque controlled by soleus muscle activation.

walking with the powered ankle exoskeleton controlled by soleus EMG (Gordon and Ferris, 2007). Subjects first walked with the powered ankle assistance for at least 15 min (*Powered*). Then the soleus H-reflex was evoked at late stance during steady state powered walking. Finally, during random steps, the power was unexpectedly turned off at midstance inducing a perturbation (*Perturbed*). After recording approximately 5 steps of perturbation without the electrical stimulations, soleus H-reflex was evoked during late stance of the perturbed steps when power was unexpectedly turned off. The gait perturbations occurred randomly and were at least 12 s apart (with a range12–38 s).

2.3. Data acquisition and analysis

We collected lower body kinematics, artificial muscle force, electromyography (EMG) and ground reaction forces (GRFs) while subjects walked on a custom-constructed force-measuring split-belt treadmill at 1.25 m/s. The three-dimensional kinematic data were collected using an 8-camera video system (120 Hz, Motion Analysis Corporation, Santa Rosa, CA, USA). Artificial muscle force data were collected with force transducers (1200 Hz, Omega Engineering, Stamford, CT, USA) mounted on the bracket of the exoskeleton. We estimated the mechanical torque, power and work done by the exoskeleton with the measurement of artificial muscle moment arm and ankle kinematic data. We placed bipolar surface electrodes on the left shank to record EMGs (1200 Hz, Konigsberg Instruments Inc., Pasadena, CA, USA) from tibialis anterior (TA), soleus (SOL), medial gastrocnemius (MG) and lateral gastrocnemius (LG). We used commercial software (Visual3D, C-Motion Inc., Germantown, MD, USA) to calculate joint angles and kinetics by inverse dynamics analysis. Lower limb inertial properties were estimated based on anthropometric measurements of subjects (Zatsiorsky, 2002) and the exoskeleton mass. We also determined when the soleus EMG and ankle angle patterns during the perturbed steps started to deviate from the patterns during the unperturbed steps (mean ± 1 standard deviation).

2.4. Soleus H-reflex measurements

We measured the soleus H-reflex in eight out of the eleven subjects. We elicited the soleus H-reflex by stimulating (DS7AH constant current stimulator, Digitimer Ltd., Hertfordshire, England) the tibial nerve with a cathode placed in the popliteal fossa and an anode (7 cm diameter) on the patella. The electrical stimulus was a 1 ms monophasic square pulse. To locate the optimal nerve stimulation site, we delivered a couple of stimuli on different spots within the popliteal fossa while subjects were standing motionless with the ankle exoskeleton unpowered. The criterion for choosing the site of cathode placement was the largest peak-to-peak amplitude of M-wave at a constant intensity of stimulation.

We recorded the soleus H-reflex during constantly powered walking (powered) and during the steps when power was unexpectedly turned off at midstance (perturbed). We divided the gait cycle into 16 equal epochs (~10 epochs during stance). We evoked soleus H-reflex at late stance (epoch 8) by which point the robotic ankle assistance started to diminish. Epoch 8 is also about the time when soleus activity reached to its peak amplitude. We used a custom-written program and a real-time control board (dSPACE Inc.) to control the timing of electrical stimulations and to measure the resulting M-wave and H-wave peak-to-peak amplitudes (2000 Hz).

The size of the M-wave as a percentage of the maximal M-wave (i.e., M_{max}, maximal evoked muscle response) has been regularly used to control constant effective stimulus intensity to the afferent nerve (Capaday, 1997; Simonsen and Dyhre-Poulsen, 1999; Ferris et al., 2001). While walking, we first collected 3 M_{max} measurements at epoch 8 by delivering a larger stimulus than the one which evoked M_{max} during quiet standing. The stimulus intensity delivered to the tibial nerve for the H-reflex measurements was the intensity which evoked a corresponding M-wave that was 25% of M_{max} for epoch 8. The program monitored the peak-to-peak amplitude of the M-wave produced by the stimulus, and calculated the ratio of the M-wave amplitude to the M_{max} for epoch 8. We only accepted H-reflex measurements where the M-wave was $25 \pm 10\%$ of the M_{max} at epoch 8. To ensure constant stimulus intensity, we manually adjusted the intensity of subsequent stimuli if the ratio was not within the acceptable range. We collected 10 measurements of H-reflex where the corresponding M-wave was $25 \pm 10\%$ of M_{max} in epoch 8.

Since the H-reflex amplitude depends on the background level of motor activity (Capaday and Stein, 1987; Capaday, 1997), we calculated the ratio of H-reflex amplitude to its corresponding background EMG amplitude. The background activity of the soleus EMG was estimated from the mean value of the rectified averaged soleus EMG during the second half (35 ms) of epoch 7 (~70 ms before the tibial nerve stimulus).

2.5. Statistics

We performed multiple paired *t*-tests to detect differences in the primary variables between the two conditions (powered versus perturbed). The primary variables were ankle positive and negative work, peak ankle moment, ankle angle at late stance, the second peak of overall support moment and of vertical GRF in the trailing leg, the first peak of vertical GRF in the contralateral leading leg and the ratio of soleus H-reflex amplitude to the background EMG. We set the significance level at $p < 0.05$ and used Bonferroni correction. All statistical analyses were performed in JMP statistical software (SAS institute Inc., Cary, NC, USA).

3. Results

Subjects reacted to the unexpectedly decreased exoskeleton plantar flexor assistance by increasing soleus muscle activation within the perturbed step to recover from the perturbation. During steady-state powered walking, the ankle exoskeleton provided a substantial plantar flexor moment (0.77 ± 0.26 Nm/kg, mean ± SD) that was ~50% of the net ankle plantar flexor

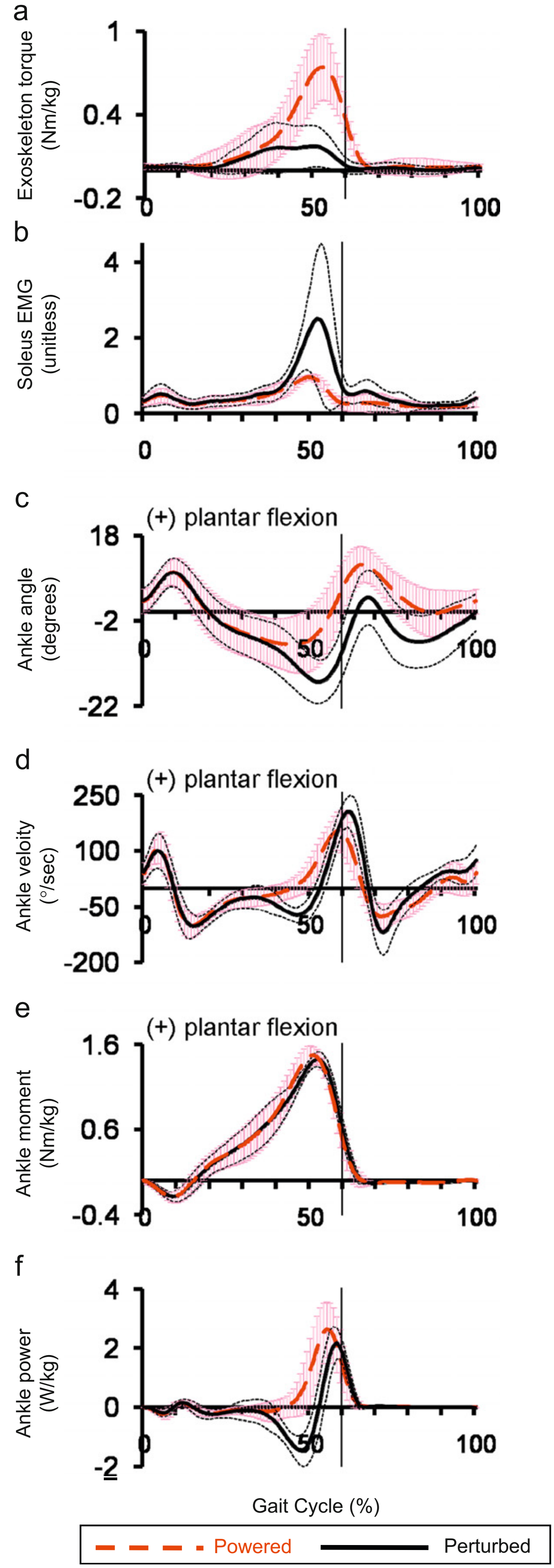

Fig. 2. Ankle joint kinematics and kinetics during constantly powered versus perturbed conditions. Ankle profiles are shown for the powered (red dashed line, mean ± 1 SD) and perturbed steps (black solid line, mean ± 1 SD). The vertical lines represent the toe-off. Positive values indicate plantar flexion. Data are the average of all subjects. The time lag between the deviated ankle angle pattern and increased soleus EMG during the perturbed steps was determined for each subject, individually. When the control signals was turned off at midstance, the mechanical torque provided by the ankle exoskeleton was reduced largely for the rest of the stance (a). The unexpected reduction in the ankle exoskeleton assistance resulted in a more dorsiflexed ankle posture (c), greater angular velocity towards dorsiflexion (d) and quickly increased soleus EMG activation (b). As a result of quick increase in soleus EMG, subjects had similar ankle moment profiles (e). Thus, due to the differences in ankle kinematics, subjects had greater power absorption and less power generation during the perturbed steps (f). (For interpretation of the references to colour in this figure legend, the reader is referred to the web version of this article.)

moment during push-off (1.50 ± 0.12 Nm/kg) (Fig. 2a and e). When exoskeleton power was turned off unexpectedly, subjects reacted quickly by increasing soleus (Fig. 2b) and other shank muscle activation (Fig. 3) for the second half of stance. The soleus EMG pattern during perturbed steps deviated from the soleus EMG pattern during powered steps (mean+1SD) with a time lag of 60 ± 29 (mean $\pm$ SD) milliseconds after the ankle angle deviated from the pattern of powered steps (mean$-$1SD). The majority of subjects had a time lag of less than 60 ms. Only two out of the eleven subjects had a longer time lag (90 and 133 ms, individually).

The ankle moment pattern during the perturbed steps was remarkably similar to the ankle moment pattern during unperturbed steps (Fig. 2e) as a result of rapid increase in soleus EMG (peak plantar flexor moment; perturbed: 1.43 ± 0.09 Nm/kg; powered: 1.50 ± 0.12 Nm/kg; *t*-test, p=0.13). There were noticeable differences in the ankle joint angle (Fig. 2c), ankle joint velocity (Fig. 2d) and ankle power (Fig. 2f) profiles during the perturbed versus powered steps. During perturbed steps, subjects had a more dorsiflexed ankle posture by $\sim 8^\circ$ (peak dorsiflexion; perturbed: $-16.64^\circ \pm 5.09^\circ$; powered: $-8.35^\circ \pm 6.75^\circ$; $p < 0.0001$), greater angular velocity towards dorsiflexion at late stance, and smaller ankle plantar flexion at toe-off by $\sim 8^\circ$ (peak plantar flexion; perturbed: $3.75^\circ \pm 6.29^\circ$; powered: $11.66^\circ \pm 4.21^\circ$, $p < 0.0001$). Due to the differences in ankle kinematics (Fig. 2c and d), subjects had different ankle power profiles between powered and perturbed steps. Subjects had significantly smaller ankle positive work (mean $\pm$ SD; perturbed: 14.6 ± 3.4 J; powered: 24.5 ± 3.4 J; $p < 0.0001$) and greater negative work (perturbed: -17.4 ± 4.7 J; powered: -8.3 ± 3.6 J; $p < 0.0001$) during the perturbed steps.

When ankle exoskeleton assistance was reduced during the random perturbed steps, subjects demonstrated notably different overall support moment profiles along with an increased knee extensor moment and delayed hip flexor moment (Fig. 4). The second peak of the overall support moment was $\sim$36% more for

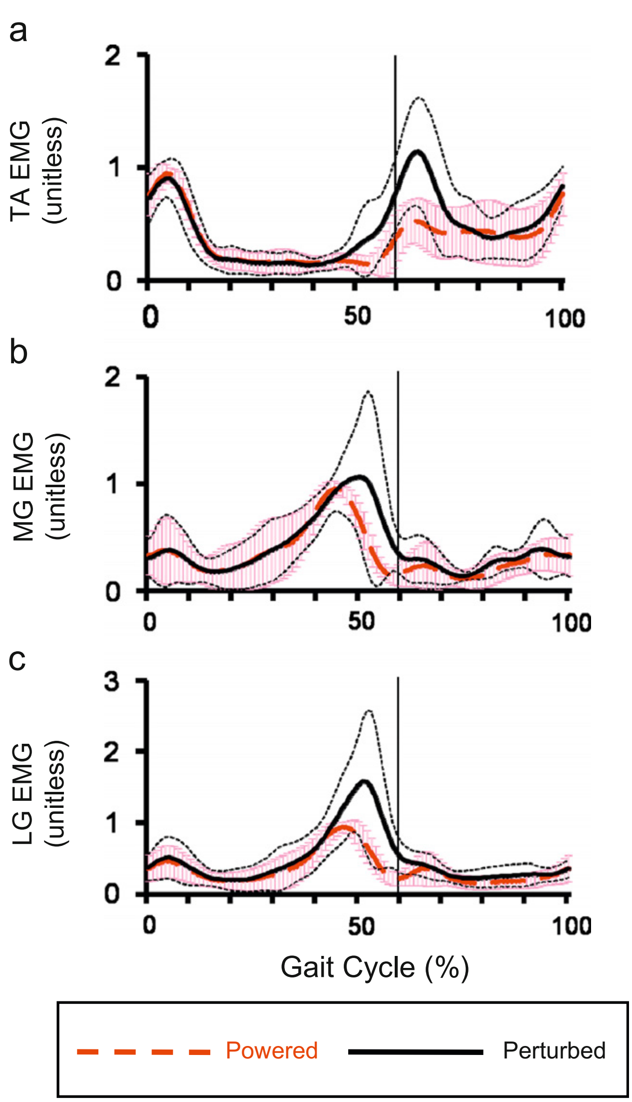

Fig. 3. Other shank muscle activation patterns. Tibialis anterior (TA), medial gastrocnemius (MG) and lateral gastrocnemius (LG) EMG profiles during powered (red dashed line, mean $\pm$ 1 SD) and perturbed steps (black solid line, mean $\pm$ 1 SD). Data were averaged for all subjects. All muscles were increased in amplitude following the perturbation. (For interpretation of the references to colour in this figure legend, the reader is referred to the web version of this article.)

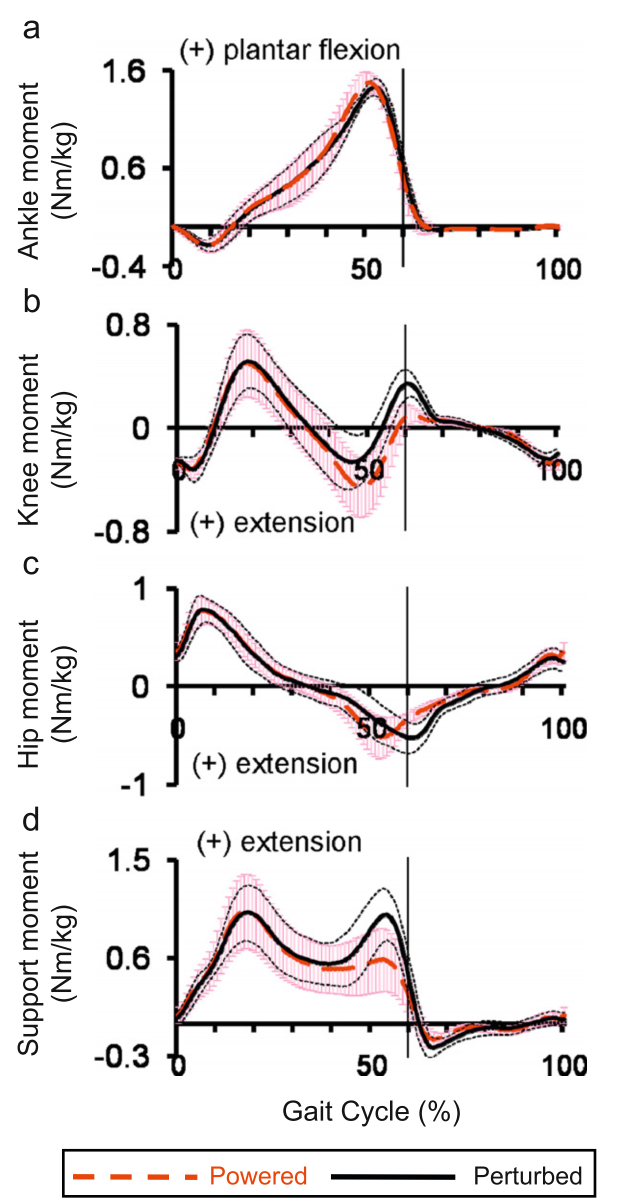

Fig. 4. Joint moments and overall support moment during powered (red dashed line, mean $\pm$ 1 SD) and perturbed steps (black solid line, mean $\pm$ 1 SD). The overall support moment (d) is the sum of extensor moments from hip (c), knee (b) and ankle (a) joints during stance. During perturbed steps, subjects had significantly different overall support moment at push-off with similar ankle plantar flexor moment, greater knee extensor moment and delayed hip flexor moment. (For interpretation of the references to colour in this figure legend, the reader is referred to the web version of this article.)

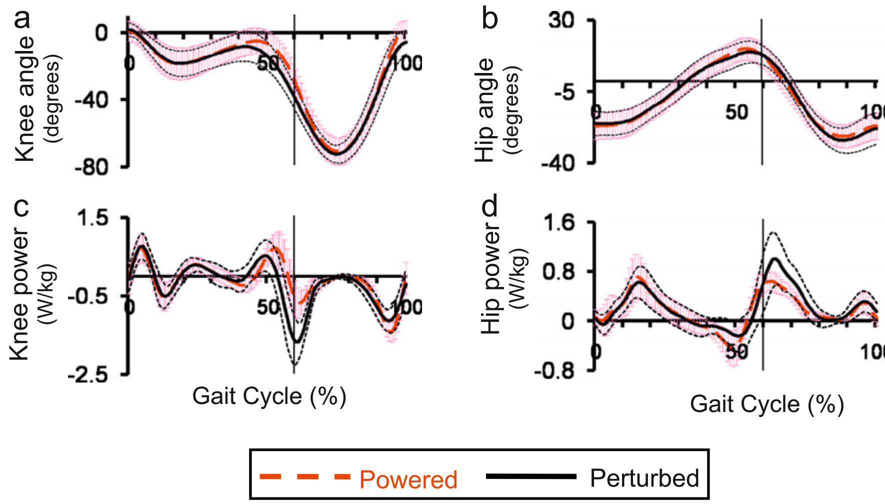

Fig. 5. Knee and hip joint angle and power profiles during powered (red dashed line, mean ± 1 SD) and perturbed steps (black solid line, mean ± 1 SD). Positive angles indicate knee extension and hip extension. During the perturbed steps, subjects had more flexed knee posture that resulted in greater knee joint power absorption, and then had greater hip joint power generation following the perturbation. (For interpretation of the references to colour in this figure legend, the reader is referred to the web version of this article.)

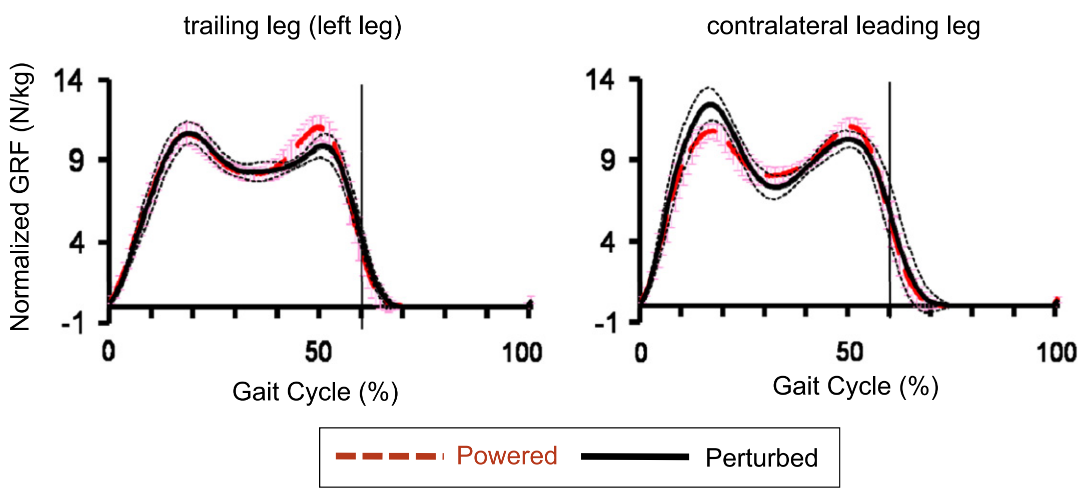

Fig. 6. Vertical ground reaction forces (GRFs) of trailing leg and the contralateral leading leg during powered (red dashed line, mean ± 1 SD) and perturbed steps (black solid line, mean ± 1 SD). When the mechanical assistance was turned off at midstance (i.e., perturbed steps), the second peak of vertical GRF in the trailing leg was reduced by ~11%. The first peak of vertical GRF in the contralateral leading leg was increased by ~15% following the perturbed steps compared to following the constantly powered steps. (For interpretation of the references to colour in this figure legend, the reader is referred to the web version of this article.)

the perturbed steps compared to the powered steps (perturbed: 1.00 ± 0.24 Nm/kg; powered: 0.64 ± 0.26 Nm/kg; $p < 0.0001$). Correspondingly, during the perturbed steps, subjects had a greater knee power absorption (perturbed: −1.77 ± 0.52 W/kg; powered: −0.84 ± 0.19 W/kg) due to a more flexed knee posture at late stance (Fig. 5). Although subjects walked with similar hip joint angle profiles, the delayed hip flexor moment during perturbed steps resulted in a delayed but increased hip flexion velocity and thus, an increase in hip joint power generation following the perturbation (perturbed: 1.09 ± 0.48 W/kg; powered: 0.70 ± 0.12 W/kg) (Fig. 5).

Despite the similarity in the ankle moment magnitude, there were differences in vertical GRFs and the center of pressure (COP) location relative to the ankle between conditions. The second peak of the vertical GRF in the trailing leg was ~11% less for the perturbed steps compared to the powered steps (perturbed: 9.93 ± 0.71 N/kg; powered: 11.13 ± 0.88 N/kg; p=0.0003) (Fig. 6). The first peak of the vertical GRF in the contralateral leading leg was ~15% greater following the perturbed steps compared to following the powered steps (perturbed: 12.53 ± 0.97 N/kg; powered: 10.93 ± 0.43 N/kg; $p < 0.0001$). Correspondingly, in the trailing leg, all subjects had greater anteroposterior distance between their center of pressure (COP) and the ankle joint location at late stance in the perturbed condition compared to the powered condition (at 50% of gait cycle: powered 8.86 ± 1.26 cm, perturbed 9.58 ± 1.23 cm, p=0.0016). The greater distance between the COP and ankle locations at late stance was likely related to the dorsiflexed ankle posture. The greater distance also explains the similar ankle moments despite a smaller vertical GRF peak during the perturbed steps compared to the powered steps.

3.1. H-reflex amplitude

Subjects had slightly higher H-reflex amplitude during the perturbed steps than during the control steps (perturbed: 28.3 ± 18.8% of M_{max}; powered: 21.8 ± 16.2% of M_{max}; p=0.117). However, background soleus EMG was also higher for the perturbed steps compared to the powered steps (perturbed: $1.6 \pm 0.7\%$ of M_{max}; powered: $1.0 \pm 0.2\%$ of M_{max}; $p = 0.055$). As a result, when normalizing H-reflex to the background soleus EMG, there was no significant difference between conditions (perturbed: 26.21 ± 22.29; powered: 23.06 ± 19.67; $p = 0.404$).

4. Discussion

When encountering an unexpected decrease in mechanical assistance from a powered ankle exoskeleton at midstance, subjects reacted quickly by rapidly increasing soleus muscle activation. Compared to the unperturbed steps, subjects had similar soleus H-reflex amplitude in proportion to the soleus background EMG during the perturbed steps. This indicates that the perturbation did not alter the reflex gain from what was normally set during steady-state walking.

The rapid response to the perturbation produced an ankle joint moment profile that was almost identical to the unperturbed control condition. However, there was a different overall support moment pattern due to a greater knee extensor moment and delayed hip flexor moment. This was also true using an alternative calculation for the support moment (Hof, 2000) although we did not present the data due to space constraints. Thus, contrary to past studies (Winter, 1980; Winter, 1989), the overall support moment pattern may not be as invariant during human gait as suggested. Our results are the first to demonstrate that the nervous system sets reflex gain during human walking to produce invariant ankle joint moment patterns in the event of a gait perturbation. While we only examined a single type of perturbation (i.e. increased dorsiflexion), the general principle of an invariant ankle joint moment pattern may hold true for other perturbations as well. Future studies should examine joint kinetics for the ankle and other lower limb joints under different perturbation paradigms (e.g. unexpectedly stepping on a raised surface).

The decrease in ankle work by the trailing limb resulted in a significantly greater collision in the contralateral leading leg. This finding supports the predictions of simple walking models that ankle push-off during human walking is a critical factor in generating an efficient gait. The powered walking model by Kuo (2002) demonstrated an increased energy loss at heel strike in the leading leg when decreasing ankle push-off energy input to the trailing leg (Kuo, 2002). Moreover, when the amount of collision exceeds the amount of ankle push-off, additional positive work must be then performed during single support to maintain a steady walking speed (Kuo et al., 2005). This additional positive work may be performed by active hip torque and is very costly (Kuo, 2002). Individuals with pathological gaits usually demonstrate insufficient muscle strength and low ankle plantar flexor muscle activation (Nadeau et al., 1999; Chen et al., 2005; Den Otter et al., 2007; Lamontagne et al., 2007; Turns et al., 2007; Chen and Patten, 2008). To improve walking efficiency, training individuals with pathological gaits to increase push-off from the trailing limb could greatly improve their walking energetics (Sawicki et al., 2009).

While there have been numerous computer simulations of musculoskeletal models for human walking, few have included reflexes or the ability to respond to perturbations. Computer simulations are a powerful tool to increase our understanding of neural and biomechanical mechanisms involved in human locomotion. Implementing components of reflex responses to simulation models is particularly useful for identifying the specific roles of sensory feedback in regulating muscle activity (Ekeberg and Pearson, 2005; Pearson et al., 2006). However, most model simulations have focused on steady state locomotion. To adequately model human movement during situations that could cause musculoskeletal injury, it is important to adequately include reflex dynamics in the simulations.

As one example, Jo (2007) successfully implemented reflexes involved in controlling leg swing trajectory during a perturbation. The result was a fairly accurate kinematic response (Jo, 2007). When encountering a gait perturbation during stance, kinetic information is likely to be more helpful in faithfully reproducing body dynamics during the perturbation. Our results demonstrated that the nervous system modulates reflex responses to maintain a consistent joint moment pattern in the event of ankle joint perturbations. Implementing a similar type of reflex scaling in neuromusculoskeletal computer simulation models could help to improve the fidelity of the simulations for studying a wider range of movement dynamics. If future experiments also document a prioritization of joint moment profiles in response to other perturbations, a general reflex scaling principle could be used for the simulations.

Conflict of interest statement

There are no conflicts of interest in this work.

Acknowledgments

The authors thank Danielle Sandella, Kristin Carroll, Evelyn Anaka, and members of the Human Neuromechanics Laboratory for assistance in collecting data. We also thank Anne Manier for help with fabricating the exoskeleton. Supported by NIH R21 NS062119 (DPF) and F32 HD055010 (CLL).

References

af Klint, R., Nielsen, J.B., Cole, J., Sinkjaer, T., Grey, M.J., 2008. Within-step modulation of leg muscle activity by afferent feedback in human walking. Journal of Physiology—London 586 (19), 4643–4648.
af Klint, R., Nielsen, J.B., Sinkjaer, T., Grey, M.J., 2009. Sudden drop in ground support produces force-related unload response in human overground walking. Journal of Neurophysiology 101 (4), 1705–1712.
Capaday, C., 1997. Neurophysiological methods for studies of the motor system in freely moving human subjects. Journal of Neuroscience Methods 74 (2), 201–218.
Capaday, C., Stein, R.B., 1987. Difference in the amplitude of the human soleus H reflex during walking and running. Journal of Physiology (London) 392, 513–522.
Chen, G., Patten, C., 2008. Joint moment work during the stance-to-swing transition in hemiparetic subjects. Journal of Biomechanics 41 (4), 877–883.
Chen, G., Patten, C., Kothari, D.H., Zajac, F.E., 2005. Gait differences between individuals with post-stroke hemiparesis and non-disabled controls at matched speeds. Gait & Posture 22 (1), 51–56.
Den Otter, A.R., Geurts, A.C.H., Mulder, T., Duysens, J., 2007. Abnormalities in the temporal patterning of lower extremity muscle activity in hemiparetic gait. Gait & Posture 25 (3), 342–352.
Ekeberg, O., Pearson, K., 2005. Computer simulation of stepping in the hind legs of the cat: an examination of mechanisms regulating the stance-to-swing transition. Journal of Neurophysiology 94 (6), 4256–4268.
Ferris, D.P., Aagaard, P., Simonsen, E.B., Farley, C.T., Dyhre-Poulsen, P., 2001. Soleus H-reflex gain in humans walking and running under simulated reduced gravity. Journal of Physiology (London) 530 (1), 167–180.
Ferris, D.P., Gordon, K.E., Sawicki, G.S., Peethambaran, A., 2006. An improved powered ankle-foot orthosis using proportional myoelectric control. Gait and Posture 23 (4), 425–428.
Gilchrist, L.A., Winter, D.A., 1997. A multisegment computer simulation of normal human gait. IEEE Transactions on Rehabilitation Engineering 5 (4), 290–299.
Gordon, K.E., Ferris, D.P., 2007. Learning to walk with a robotic ankle exoskeleton. Journal of Biomechanics 40 (12), 2636–2644.
Hof, A.L., 2000. On the interpretation of the support moment. Gait Posture 12 (3), 196–199.
Jo, S., 2007. A neurobiological model of the recovery strategies from perturbed walking. Biosystems 90 (3), 750–768.
Kuo, A.D., 2002. Energetics of actively powered locomotion using the simplest walking model. Journal of Biomechanical Engineering 124 (1), 113–120.
Kuo, A.D., Donelan, J.M., Ruina, A., 2005. Energetic consequences of walking like an inverted pendulum: step-to-step transitions. Exercise and Sport Sciences Reviews 33 (2), 88–97.

Lamontagne, A., Stephenson, J.L., Fung, J., 2007. Physiological evaluation of gait disturbances post stroke. Clinical Neurophysiology 118 (4), 717–729.
Mazzaro, N., Grey, M.J., Sinkjaer, T., 2005a. Contribution of afferent feedback to the soleus muscle activity during human locomotion. Journal of Neurophysiology 93 (1), 167–177.
Mazzaro, N., Grey, M.J., Sinkjaer, T., Andersen, J.B., Pareyson, D., Schieppati, M., 2005b. Lack of on-going adaptations in the soleus muscle activity during walking in patients affected by large-fiber neuropathy. Journal of Neurophysiology 93 (6), 3075–3085.
Nadeau, S., Gravel, D., Arsenault, A.B., Bourbonnais, D., 1999. Plantarflexor weakness as a limiting factor of gait speed in stroke subjects and the compensating role of hip flexors. Clinical Biomechanics 14 (2), 125–135.
Nielsen, J.B., Sinkjaer, T., 2002. Afferent feedback in the control of human gait. Journal of Electromyography and Kinesiology 12 (3), 213–217.
Pandy, M.G., 2001. Computer modeling and simulation of human movement. Annual Review of Biomedical Engineering 3, 245–273.
Pearson, K., Ekeberg, O., Buschges, A., 2006. Assessing sensory function in locomotor systems using neuro-mechanical simulations. Trends in Neurosciences 29 (11), 625–631.
Rossignol, S., Dubuc, R.J., Gossard, J.P., 2006. Dynamic sensorimotor interactions in locomotion. Physiological Reviews 86 (1), 89–154.
Sawicki, G.S., Ferris, D.P., 2008. Mechanics and energetics of level walking with powered ankle exoskeletons. Journal of Experimental Biology 211 (9), 1402–1413.
Sawicki, G.S., Lewis, C.L., Ferris, D.P., 2009. It pays to have a spring in your step. Exercise and Sport Sciences Reviews 37 (3), 130–138.
Simonsen, E.B., Dyhre-Poulsen, P., 1999. Amplitude of the human soleus H reflex during walking and running. Journal of Physiology—London 515 (3), 929–939.
Sinkjaer, T., Andersen, J.B., Larsen, B., 1996. Soleus stretch reflex modulation during gait in humans. Journal of Neurophysiology 76 (2), 1112–1120.
Turns, L.J., Neptune, R.R., Kautz, S.A., 2007. Relationships between muscle activity and anteroposterior ground reaction forces in hemiparetic walking. Archives of Physical Medicine and Rehabilitation 88 (9), 1127–1135.
Winter, D.A., 1980. Overall principle of lower limb support during stance phase of gait. Journal of Biomechanics 13 (11), 923–927.
Winter, D.A., 1989. Biomechanics of normal and pathological gait—implications for understanding human locomotor control. Journal of Motor Behavior 21 (4), 337–355.
Yang, J.F., Stein, R.B., James, K.B., 1991. Contribution of peripheral afferents to the activation of the soleus muscle during walking in humans. Experimental Brain Research 87 (3), 679–687.
Zatsiorsky, V.M., 2002. Kinetics of Human Motion. Human Kinetics.